Available online at www.sciencedirect.com
ScienceDirect
Bioorganic & Medicinal Chemistry Letters 17 (2007) 3161–3166
Bioorganic & Medicinal Chemistry Letters

Structure function analysis of benzalacetone synthase from *Rheum palmatum*

Tsuyoshi Abe,[a] Hiroyuki Morita,[b] Hisashi Noma,[a] Toshiyuki Kohno,[b] Hiroshi Noguchi[a] and Ikuro Abe[a,c,*]

[a]*School of Pharmaceutical Sciences, The COE21 Program, University of Shizuoka, 52-1 Yada, Shizuoka 422-8526, Japan*
[b]*Mitsubishi Kagaku Institute of Life Sciences (MITILS), Machida, Tokyo 194-8511, Japan*
[c]*PRESTO, Japan Science and Technology Agency, Kawaguchi, Saitama 332-0012, Japan*

Received 30 January 2007; revised 7 March 2007; accepted 10 March 2007
Available online 15 March 2007

Abstract—Benzalacetone synthase (BAS) is a plant-specific chalcone synthase (CHS) superfamily type III polyketide synthase (PKS) that catalyzes a one-step decarboxylative condensation of 4-coumaroyl-CoA with malonyl-CoA. The diketide forming activity of *Rheum palmatum* BAS is attributed to the characteristic substitution of the conserved active-site Phe215 with Leu (numbering in *Medicago sativa* CHS). To further understand the structure and function of *R. palmatum* BAS, four site-directed mutants (C197T, C197G, G256L, and S338V) were newly constructed. All the mutants did not change the product pattern, however, the activity was 2-fold increased in S338V, while reduced to half in G256L mutant. On the other hand, the C197 mutants were functionally almost identical to wild-type BAS, excluding the possibility that the second active-site Cys is involved in the enzyme reaction. Instead, homology modeling suggested a possibility that, unlike the case of CHS, BAS utilizes an alternative pocket to lock the coumaroyl moiety for the diketide formation reaction.

Benzalacetone synthase (BAS) (EC 2.3.1.-) is a plant-specific chalcone synthase (CHS) superfamily of type III polyketide synthases (PKSs)[1,2] that catalyzes one-step decarboxylative condensation of 4-coumaroyl-CoA with malonyl-CoA to produce a diketide benzalacetone, 4-(4-hydroxyphenyl)but-3-en-2-one (Fig. 1a).[3,4] BAS is thought to play a crucial role for construction of the C_6–C_4 moiety of a variety of medicinally important phenylbutanoids such as anti-inflammatory glucoside lindleyin in rhubarb, gingerol, and curcumin in ginger plants, and raspberry ketone, the characteristic aroma of raspberry fruits.[3] On the other hand, CHS (EC 2.3.1.74), sharing ca. 70% amino acid sequence identity with BAS, performs sequential condensations of 4-coumaroyl-CoA with three C_2 units from malonyl-CoA to produce a tetraketide naringenin chalcone (4,2′,4′,6′-tetrahydroxychalcone) (Fig. 1c), which is the biosynthetic precursor of flavonoids.[1,2]

In the previous work, we reported that the diketide-forming activity of *Rheum palmatum* (Polygonaceae) BAS is derived from the characteristic substitution of the CHS active-site Phe215; the conserved residues ^{214}LF are uniquely replaced by IL in BAS (numbering in *Medicago sativa* CHS).[3,4] The conformationally flexible Phe215, located at the junction between the active-site cavity and the CoA binding tunnel, is absolutely conserved in all the known type III PKSs, and thought to facilitate decarboxylation of malonyl-CoA; help orient substrates and intermediates during the sequential condensation reactions.[5,6] Our observation that *R. palmatum* BAS I214L/L215F mutant restored chalcone-forming activity supported a hypothesis that the absence of Phe215 in BAS accounts for the interruption of the polyketide chain elongation at the diketide stage.[4]

On the other hand, another interesting feature of the diketide-producing *R. palmatum* BAS is that CHS's conserved active-site Thr197, the important residue for steric modulation of the active-site in a number of divergent type III PKSs, is uniquely replaced with reactive Cys (Fig. 2).[4] Interestingly, Austin and Noel proposed a hypothesis that BAS utilizes this second active-site Cys for the decarboxylation reaction of a diketide

Keywords: Benzalacetone synthase; Chalcone synthase; Type III polyketide synthase; Benzalacetone; Engineered biosynthesis.
* Corresponding author. Tel./fax: +81 54 264 5662; e-mail: abei@ys7.u-shizuoka-ken.ac.jp

0960-894X/$ - see front matter © 2007 Elsevier Ltd. All rights reserved.
doi:10.1016/j.bmcl.2007.03.029

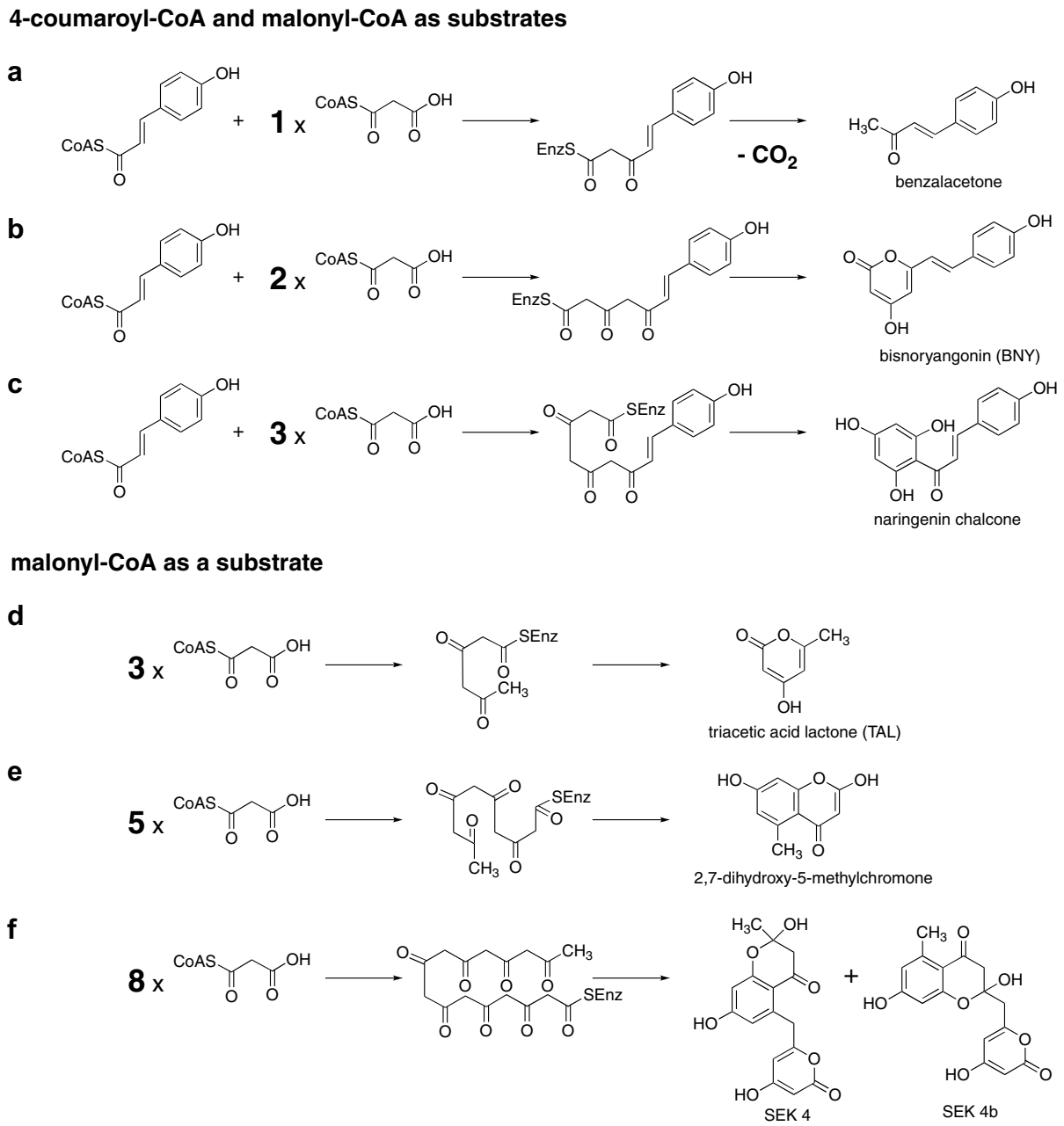

Figure 1. Proposed mechanism for the formation of (a) benzalacetone (BA), (b) bisnoryangonin (BNY), and (c) naringenin chalcone, from 4-coumaroyl-CoA and malonyl-CoA as substrates. Formation of (d) triacetic acid lactone (TAL), (e) 5,7-dihydroxy-2-methylchromone, and (f) SEK4 and SEK4b, from malonyl-CoA as a substrate.

intermediate to produce benzalacetone.[2] To test the hypothesis, here we constructed a mutant in which Cys197 (numbering in CHS) is substituted with Thr and investigated the mechanistic consequence of the point mutation. In addition, to further study the structure and function of *R. palmatum* BAS, we also constructed mutants in which the active-site Cys197, Gly256, and Ser338 (numbering in CHS) were, respectively, replaced with Gly, Leu, and Val, as in the case of the recently reported *Aloe arborescens* octaketide synthase (OKS), a novel CHS-superfamily type III PKS that produces octaketides SEK4 and SEK4b from eight molecules of malonyl-CoA (Fig. 1f).[7] The large-to-small C197G and the OKS-like bulky G256L replacements are thought to be important for steric modulation of the active-site architecture, thereby affecting substrate and product specificity of the enzyme reaction.[7–12] Very interestingly, it has been recently reported that S338V mutant of *Scutellaria baicalensis* CHS produced a trace amount of octaketides SEK4 and SEK4b by the simple steric modulation of the chemically inert single residue lining the active-site cavity.[9]

All the mutants were expressed in *Escherichia coli* at levels comparable with wild-type enzyme and purified to homogeneity by a Ni-chelate affinity column.[13,14] Interestingly, the replacement of Cys197 with Thr or Gly did not significantly affect the enzyme activity;[15] both

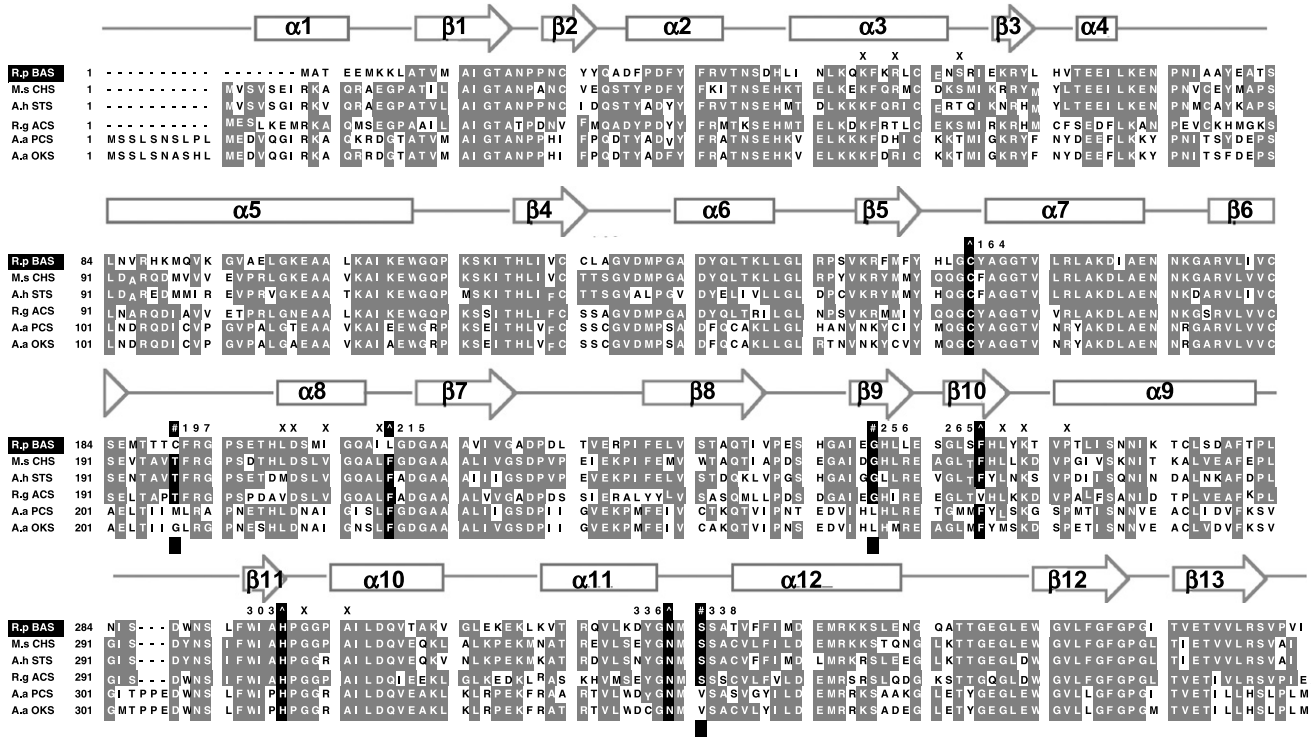

Figure 2. Sequence alignment of *Rheum palmatum* BAS and other CHS-superfamily type III PKSs: R.p BAS, *R. palmatum* benzalacetone synthase; M.s CHS, *Medicago sativa* CHS; A.h STS, *Arachis hypogaea* stilbene synthase; R.g ACS, *Ruta graveolens* acridone synthase; A.a PCS, *Aloe arborescens* PCS; A.a OKS, *A. arborescens* OKS. The catalytic triad (Cys164, His303, and Asn336) and the gatekeeper Phes (Phe215 and Phe265) are marked with ^, and the active-site residues 197, 256, and 338 with # (numbering in *M. sativa* CHS). Residues for the CoA binding are marked with X. α-Helices (rectangles) and β-strands (arrows) of CHS are diagrammed.

C197T and C197G mutant were functionally almost identical to wild-type BAS, and efficiently produced BA after condensation of 4-coumaroyl-CoA[16] with one molecule of malonyl-CoA (Fig. 1a). This demonstrated that Cys197 is not essential for the BA-producing activity, and excluded the possibility that the second active-site Cys is involved in the decarboxylation reaction of the diketide intermediate. On the other hand, G256L mutant showed 2-fold decrease, while S338V mutant showed 2-fold increase in the BA-forming activity at pH 8 (Fig. 3). Furthermore, as in the case of wild-type *R. palmatum* BAS, all the mutants afforded a triketide pyrone bisnoryangonin (BNY) after two condensations with malonyl-CoA (Fig. 1b) under acidic pH: the BA-forming activity was maximum at pH 8, while BNY was obtained as a major product at pH 6 (Fig. 3). However, formation of other products such as a tetraketide pyrone 4-coumaroyltriacetic acid lactone[17] or naringenin chalcone (Fig. 1c) was not detected for all the mutant enzymes, which indicated that the point mutations do not affect the product chain length (the number of condensations with malonyl-CoA) and the product specificity. Steady-state kinetics analysis[18] (BA-forming activity at pH 8.0) revealed that S338V mutant showed $K_M = 9.4\ \mu M$ and $k_{cat} = 3.18\ min^{-1}$ for 4-coumaroyl-CoA, while wild-type *R. palmatum* BAS showed $K_M = 10.0\ \mu M$ and $k_{cat} = 1.79\ min^{-1}$ for 4-coumaroyl-CoA. The replacement of the single residue thus led to 2-fold increase in the k_{cat}/K_M value for the BA-forming activity. It is remarkable that the turnover number (the k_{cat} value) was doubled while the K_M value remained nearly equal, implicating its potential influence on the catalytic steps that follow the substrate loading.

On the other hand, when malonyl-CoA was used as the sole substrate, both wild-type and the mutant (C197T, C197G, G256, and S338V) *R. palmatum* BAS initiated decarboxylative condensation of malonyl-CoA as a starter, and most of the polyketide chain elongation reactions were terminated at the triketide stage to predominantly produce triacetic acid lactone (TAL) (Fig. 1d). This is largely in good agreement with earlier reports on *M. sativa* CHS[11] and *S. baicalensis* CHS.[9] However, interestingly, unlike the previously reported *S. baicalensis* CHS S338V mutant, formation of octaketides SEK4 and SEK4b[9] from eight molecules of malonyl-CoA (Fig. 1f) was not detected by the LC–ESIMS analysis. Instead, *R. palmatum* BAS S338V mutant only afforded a trace amount of a pentaketide 2,7-dihydroxy-5-methylchromone[9] from five molecules of malonyl-CoA (Fig. 1e). According to the homology models as discussed below, *R. palmatum* BAS mutants seem to have enough space for the octaketide formation reaction in the active-site cavity (Fig. 4). The observed result would reflect the subtle structural differences between the two enzymes.

In the absence of a crystal structure of *R. palmatum* BAS, homology models[19] were constructed on the basis of the crystal structure of *M. sativa* CHS (PDB code: 1BQ6A)[5] (Fig. 4). The model predicted that *R. palmatum* BAS has the same overall fold as *M. sativa* CHS, with a

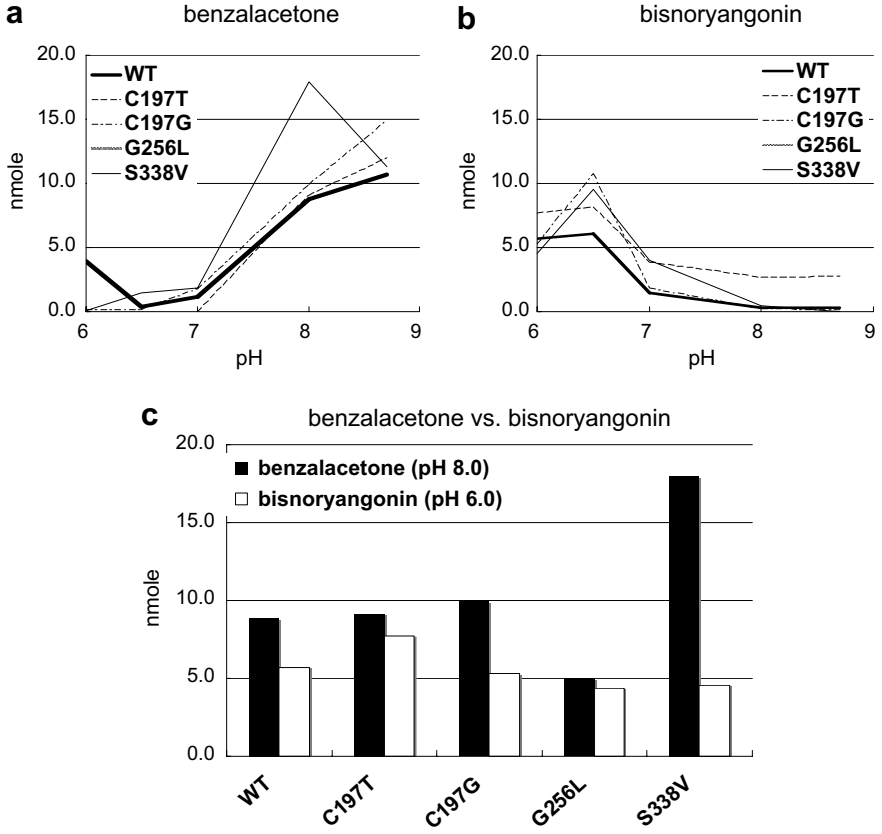

Figure 3. The pH dependence of (a) benzalacetone and (b) bisnoryangonin production by wild-type BAS and its mutants in 100 mM potassium phosphate buffer. (c) Production of benzalacetone (at pH 8.0) and bisnoryangonin (at pH 6.0) by *R. palmatum* BAS and its mutants. The reaction mixture contained 27 μM of 4-coumaroyl-CoA, 54 μM of malonyl-CoA, and 20 μg of the purified enzyme in a final volume of 500 μL of 100 mM potassium phosphate buffer.

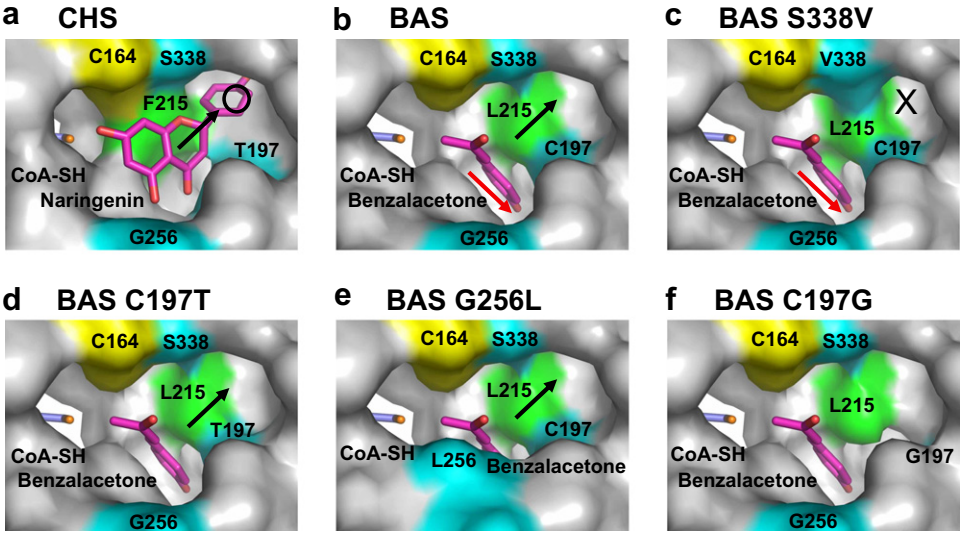

Figure 4. Homology models of *R. palmatum* BAS and its mutants. The active-site cavity of (a) *M. sativa* CHS, (b) *R. palmatum* BAS, (c) BAS S338V mutant, (d) BAS C197T mutant, (e) BAS G256L mutant, and (f) BAS C197G mutant. CoA, naringenin, and benzalacetone molecules are shown in *stick* representation. The 'coumaroyl binding pocket'[5] is indicated by a black arrow, while the proposed alternative pocket for BA-production is indicated by a red arrow.

cavity volume estimated to be 881 Å^3, which is smaller than that of *M. sativa* CHS (1019 Å^3).[4] Notably, the 'coumaroyl-binding pocket'[5] (indicated by a black arrow in Fig. 4) of BAS is apparently smaller than that of CHS. Further, as mentioned above, the CHS's gatekeeper Phe215 is characteristically replaced with non-

aromatic Leu in *R. palmatum* BAS. These structural changes would make it difficult for *R. palmatum* BAS to properly lock the coumaroyl starter in the 'coumaroyl binding pocket' during the polyketide chain elongation reaction. Instead, we propose a hypothesis that *R. palmatum* BAS utilizes an alternative pocket (indicated by a red arrow in Fig. 4) to lock the coumaroyl moiety for the diketide formation reaction.

The homology model also suggested that the hydrophobic replacement of Ser338 located next to the catalytic Cys164 further narrows the entrance of the 'coumaroyl-binding pocket' (Fig. 4c), and, as a result, provides steric guidance so that the polyketide intermediate extends into the downward alternative pocket, thereby leading to improvement of the BA-forming activity in S338V mutant. Indeed, as mentioned above, the kinetic data indicated that the point mutation led to 2-fold increase in the turnover number (the k_{cat} value), while the K_M value remained nearly equal, which would support the hypothesis. Moreover, the models also suggested that C197T and C197G mutations do not affect the volume of the alternative pocket, therefore causing no significant effects on the enzyme activity (Fig. 4d and f). On the other hand, the small-to-large G256L substitution greatly reduces the active-site cavity volume (Fig. 4e). Although it has been reported that CHS G256L mutants no longer accept the bulky coumaroyl-CoA as a starter substrate,[9,11] the situation seems to be a little different in *R. palmatum* BAS, and BAS G256L mutant still managed to accept the coumaroyl starter to produce BA, but with half of the catalytic efficiency (in this case, both the k_{cat} and the K_M values should be reduced). This result again suggested the structural differences of the active-site between CHS and *R. palmatum* BAS; presumably BAS can still utilize one of the pockets for the coumaroyl moiety loading and the diketide formation reaction (Fig. 4e).

In summary, S338V mutant exhibited 2-fold increase in the k_{cat}/K_M value for the BA-producing activity, suggesting that the residue is important for providing steric guidance of the diketide formation reaction. On the other hand, C197T and C197G mutants were functionally almost identical with wild-type BAS, which excluded the possibility that the second active-site Cys is involved in the enzyme reaction. Instead, homology modeling suggested a possibility that, unlike the case of CHS, BAS utilizes an alternative pocket to lock the coumaroyl moiety for the diketide formation reaction. These results provided structural insights into the functional diversity of type III PKS enzymes and suggest strategies for the engineered biosynthesis of plant polyketides.

Acknowledgments

This work was supported by the PRESTO program from Japan Science and Technology Agency, Grant-in-Aid for Scientific Research (Nos. 18510190 and 17310130), and the COE21 program from the Ministry of Education, Culture, Sports, Science and Technology, Japan.

References and notes

1. Schröder, J. In *Comprehensive Natural Products Chemistry*; Elsevier: Oxford, 1999; Vol. 1, pp 749–771.
2. Austin, M. B.; Noel, J. P. *Nat. Prod. Rep.* **2003**, *20*, 79.
3. Abe, I.; Takahashi, Y.; Morita, H.; Noguchi, H. *Eur. J. Biochem.* **2001**, *268*, 3354.
4. Abe, I.; Sano, Y.; Takahashi, Y.; Noguchi, H. *J. Biol. Chem.* **2003**, *278*, 25218.
5. Ferrer, J. L.; Jez, J. M.; Bowman, M. E.; Dixon, R. A.; Noel, J. P. *Nat. Struct. Biol.* **1999**, *6*, 775.
6. Jez, J. M.; Ferrer, J. L.; Bowman, M. E.; Dixon, R. A.; Noel, J. P. *Biochemistry* **2000**, *39*, 890.
7. Abe, I.; Oguro, S.; Utsumi, Y.; Sano, Y.; Noguchi, H. *J. Am. Chem. Soc.* **2005**, *127*, 12709.
8. Abe, I.; Utsumi, Y.; Oguro, S.; Morita, H.; Sano, Y.; Noguchi, H. *J. Am. Chem. Soc.* **2005**, *127*, 1362.
9. Abe, I.; Watanabe, T.; Morita, H.; Kohno, T.; Noguchi, H. *Org. Lett.* **2006**, *8*, 499.
10. Abe, I.; Watanabe, T.; Lou, W.; Noguchi, H. *FEBS J.* **2006**, *273*, 208.
11. Jez, J. M.; Austin, M. B.; Ferrer, J.; Bowman, M. E.; Schröder, J.; Noel, J. P. *Chem. Biol.* **2000**, *7*, 919.
12. Jez, J. M.; Bowman, M. E.; Noel, J. P. *Biochemistry* **2001**, *40*, 14829.
13. Site-directed mutagenesis. *R. palmatum* BAS mutants (C197T, C197G, G256L, and S338V) were constructed using the QuickChange Site-Directed Mutagenesis Kit (Stratagene) and a pair of primers as follows (mutated codons are underlined): C197T (5′-CAGAGATGACAA CAACTACTTTTCGTGGGCCATCTG-3′ and 5′-CAG ATGGCCCACGAAAAGTAGTTGTTGTCATCTCT G-3′), C197G (5′-AGATGACAACAACTGGTTTTCG TGGGCCATCT-3′ and 5′-AGATGGCCCACGAAAA CCAGTTGTTGTCATCT-3′), G256L (5′-CATGGTG CAATTGAGCTCCACTTGCTTGAATC-3′ and 5′-GA TTCAAGCAAGTGGAGCTCAATTGCACCATG-3′), and S338V (5′-GACTATGGAAACATGGTGAGC GCT ACGGTGTTTTTC-3′ and 5′-GAAAAACACCG TAGC GCTCACCATGTTTCCATAGTC-3′).
14. Enzyme expression and purification. After confirmation of the sequence, the plasmid was transformed into *E. coli* M15. The cells harboring the plasmid were cultured to an A_{600} of 0.6 in LB medium containing 100 μg/mL of ampicillin at 30 °C. Then, 1.0 mM isopropylthio-β-D-galactoside was added to induce protein expression, and the culture was incubated further at 30 °C for 16 h. The *E. coli* cells were harvested by centrifugation and resuspended in 50 mM potassium phosphate buffer, pH 8.0, containing 0.1 M NaCl. Cell lysis was carried out by the freeze–thaw method and centrifuged at 15,000*g* for 60 min. The supernatant was passed through a column of Ni Sepharose™ 6 Fast Flow (Amersham Bioscience). After washing with 50 mM potassium phosphate buffer, pH 7.9, containing 0.5 M NaCl and 40 mM imidazole, the recombinant BAS was finally eluted with 15 mM potassium phosphate buffer, pH 7.5, containing 10% glycerol and 500 mM imidazole. Finally, the enzyme preparation was desalted by Bio-Gel P6DG Desalting gel. Protein concentration was determined by the Bradford method (Protein Assay, Bio-Rad) with bovine serum albumin as standard.
15. Enzyme reaction. The standard reaction mixture contained 54 μM of 4-coumaroyl-CoA, 108 μM of malonyl-CoA, and 20 μg of the purified enzyme in a final volume of 500 μL of 100 mM potassium phosphate buffer, pH 8.0, containing 1 mM EDTA. Incubations were carried out at 30 °C for 20 min and stopped by addition of 50 μL of 20% HCl. The products were then extracted with 2 mL of ethyl

acetate. The products were separated by reverse-phase HPLC (JASCO 880) on a TSK-gel ODS-80Ts column (4.6 × 150 mm, TOSOH) with a flow rate of 0.8 mL/min. Gradient elution was performed with H_2O and MeOH, both containing 0.1% TFA: 0–5 min, 30% MeOH; 5–17 min, linear gradient from 30 to 60% MeOH; 17–25 min, 60% MeOH; 25–27 min, linear gradient from 60 to 70% MeOH. Elutions were monitored by a multichannel UV detector (MULTI 340, JASCO) at 290, 330, and 360 nm; UV spectra (198–400 nm) were recorded every 0.4 s. On-line LC–ESIMS spectra were measured with an Agilent Technologies HPLC 1100 series coupled to a Bruker Daltonics esquire4000 ion trap mass spectrometer fitted with an ESI source. HPLC separations were carried out under the same conditions as described above. The ESI capillary temperature and capillary voltage were 320 °C and 4.0 V, respectively. The tube lens offset was set at 20.0 V. All spectra were obtained in both negative and positive mode; over a mass range of *m*/*z* 50–600, at a range of one scan every 0.2 s. The collision gas was helium, and the relative collision energy scale was set at 30.0% (1.5 eV).

16. 4-Coumaroyl-CoA was chemically synthesized as described; Stöckigt, J.; Zenk, M. H. *Z. Naturforsch.* **1975**, *30c*, 352. [2-^{14}C]Malonyl-CoA (48 mCi/mmol) was purchased from Moravek Biochemicals. Malonyl-CoA was purchased from Sigma.
17. Akiyama, T.; Shibuya, M.; Liu, H.; Ebizuka, Y. *Eur. J. Biochem.* **1999**, *263*, 834.
18. Enzyme kinetics. Steady-state kinetic parameters were determined by using [2-^{14}C]malonyl-CoA (1.8 mCi/mmol) as a substrate. The experiments were carried out in triplicate using four concentrations of 4-coumaroyl-CoA (54.0, 27.0, 10.8, and 5.4 μM) in the assay mixture, containing 108 μM of malonyl-CoA, 20 μg of purified enzyme, and 1 mM EDTA, in a final volume of 500 μL of 100 mM potassium phosphate buffer. Incubations were carried out at 30 °C for 20 min. The reaction products were extracted and separated by TLC (Merck Art. 1.11798 Silica gel 60 F_{254}; ethyl acetate/hexane/AcOH = 63:27:5, v/v/v). Radioactivities were quantified by autoradiography using a bioimaging analyzer BAS-2000II (FUJIFILM). Lineweaver–Burk plots of data were employed to derive the apparent K_M and k_{cat} values (average of triplicates) using EnzFitter software (BIOSOFT).
19. Homology modeling. The models of *R. palmatum* BAS and its mutants were generated by the SWISS-MODEL package (http://expasy.ch/spdbv/) provided by the Swiss-PDB-Viewer program (Guex, N.; Peitsch, M. C. *Electrophoresis* **1997**, *18*, 2714) based on the crystal structure of *M. sativa* CHS (PDB code: 1BQ6A). The model quality was checked using PROCHECK (Liang, J.; Edelsbrunner, H.; Woodward, C. *Protein Sci.* **1998**, *7*, 1884). In the Ramachandran plot calculated for the model, most amino acid residues group in the energetically allowed regions with only few exceptions, primarily Gly residues that can adopt phi/psi angles in all four quadrants.